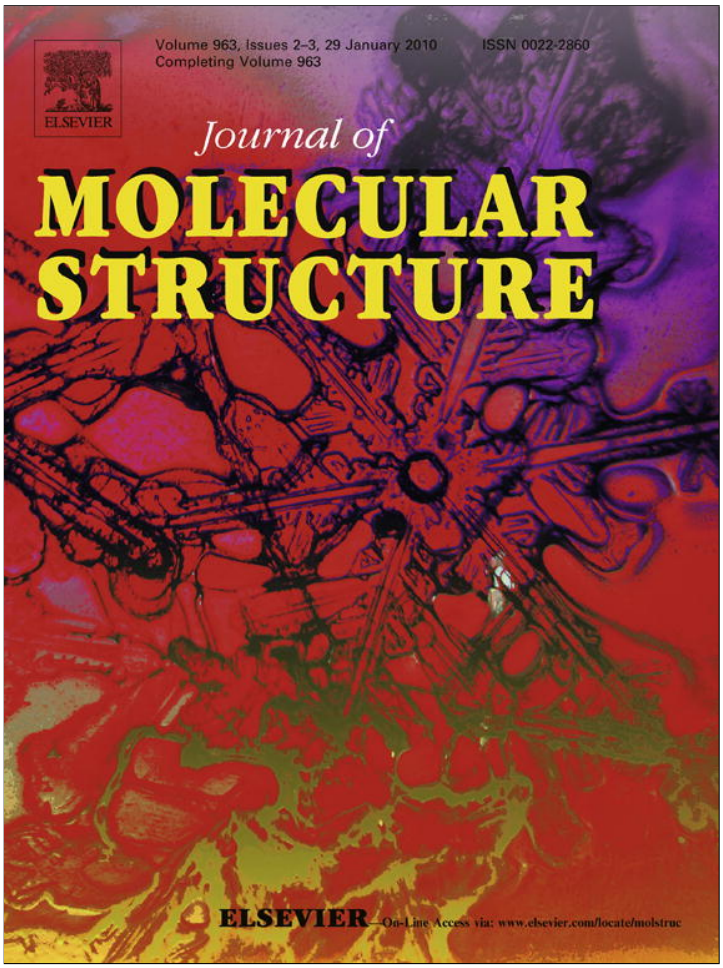

Journal of Molecular Structure 963 (2010) 122–129

Contents lists available at ScienceDirect

Journal of Molecular Structure

journal homepage: www.elsevier.com/locate/molstruc

Spectroscopic investigations of pentobarbital interaction with human serum albumin

Saqer M. Darwish [a,*], Sawsan E. Abu sharkh [a], Musa M. Abu Teir [a], Sami A. Makharza [b], Mahmoud M. Abu-hadid [c]

[a] Physics Department, Al-Quds University, P.O. Box 20002, Abu-Dies, Jerusalem, West Bank, Palestine Via, Israel
[b] Nano Technology Lab, Al-Quds University, P.O. Box 20002, Abu-Dies, Jerusalem, West Bank, Palestine Via, Israel
[c] Immunology Department, Al-Quds University, P.O. Box 20002, Abu-Dies, Jerusalem, West Bank, Palestine Via, Israel

ARTICLE INFO

Article history:
Received 8 August 2009
Received in revised form 11 October 2009
Accepted 13 October 2009
Available online 21 October 2009

Keywords:
Pentobarbital
HSA
Binding constant
Protein secondary structure
FT-IR spectroscopy

ABSTRACT

The interaction between pentobarbital and human serum albumin has been investigated. The basic binding interaction was studied by UV-absorption and fluorescence spectroscopy. From spectral analysis pentobarbital showed a strong ability to quench the intrinsic fluorescence of HSA through a static quenching procedure. The binding constant (k) is estimated at $1.812 \times 10^4\ M^{-1}$ at 293 K. FT-IR spectroscopy with Fourier self-deconvolution technique was used to determine the protein secondary structure and drug binding mechanisms. The observed spectral changes of HSA–pentobarbital complex indicate a larger intensity decrease in the absorption band of α-helix relative to that of β-sheets. This variation in intensity is related indirectly to the formation of H-bonding in the complex molecules, which accounts for the different intrinsic propensities of α-helix and β-sheets.

1. Introduction

Pentobarbital is in a class of drugs called barbiturates (Fig. 1) [1]. Barbiturates are substituted pyrimidine derivatives in which the basic structure common to these drugs is barbituric acid, a substance which has no central nervous system (CNS) activity, CNS activity is attained by substituting alkyl, alkenyl, or any groups on the pyrimidine ring. Pentobarbital is approved for human uses by the FDA for seizure and preoperative sedation. Pentobarbital has a variety of effects, including motor impairments, in both humans and animals [2]. Pentobarbital is capable of having a profound effect on brain function; it is known to depress cerebral glucose utilization and electrical activity [3].

Human serum albumin (HSA) is the most abundant protein in blood plasma and is able to bind and thereby transport, various compounds such as fatty acids, hormones, bilirubin, tryptophan, steroids, metal ions, therapeutic agents and a large number of drugs. HSA serves as the major soluble protein constituent of the circulatory system, it contributes to colloid osmotic blood pressure, it can bind and carry drugs which are poorly soluble in water [4].

The three-dimensional structure of HSA is determined through X-ray crystallographic measurements [5]. HSA consists of a single polypeptide chain of 585 amino acids. Its structure consists of three homologous domains (labeled as I, II and III), each of which is divided into two subdomains, A and B, having six and four α-helices, respectively [6].

The primary pharmacokinetics function of HSA is participating in absorption, distribution, metabolism and excretion of drugs. Drugs distribution is mainly controlled by HSA, because most drugs travel in plasma and reach the target tissues by binding to HSA [7]. It has been shown that the distribution, free concentration and the metabolism of various drugs can be significantly altered as a result of their binding to HSA [8].

The binding properties of albumin depend on the three-dimensional structure of the binding sites, which are distributed over the molecule. Strong binding can decrease the concentrations of free drugs in plasma, whereas weak binding can lead to a short lifetime or poor distribution. Its remarkable capacity to bind a variety of drugs results in its prevailing role in drug pharmacokinetics and pharmacodynamics [9]. Multiple drug binding sites have been reported for HSA by several researchers [10–16]. The principal regions of ligand binding sites of HSA are located in hydrophobic cavities in sub domains IIA and IIIA, which are corresponding to site I and site II, respectively. Site I is dominated by strong hydrophobic interaction with most neutral, bulky, heterocyclic compounds, while site II mainly by dipole–dipole, van der Waals, and/or hydrogen-bonding interactions with many aromatic car-

* Corresponding author. Tel.: +972 2 2799753; fax: +972 2 2791292.
E-mail addresses: sdarwish@science.alquds.edu (S.M. Darwish), Sabusharkh@science.alquds.edu (S.E. Abu sharkh), abuteit@science.alquds.edu (M.M. Abu Teir), smakharza@science.alquds.edu (S.A. Makharza), mabuhadid@alquds.med.edu (M.M. Abu-hadid).

0022-2860/$ - see front matter © 2009 Elsevier B.V. All rights reserved.
doi:10.1016/j.molstruc.2009.10.023

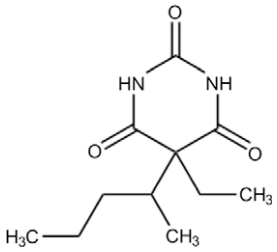

Fig. 1. Chemical structure of pentobarbital.

boxylic acids. HSA contained a single intrinsic tryptophan residue (Trp 214) in domain IIA and its fluorescence is sensitive to the ligands bounded nearby [17,18]. Therefore, it is often used as a probe to investigate the binding properties of drugs with HSA.

The modes, specificities and capacities of ligand binding to albumin are as diverse as the compounds, which can be bound [19]. The modes of binding include complex formation with metal like copper, hydrophobic and electrostatic interaction in high affinity binding and covalent binding to different amino acids. Several binding sites are distributed over the molecule according to different marker molecules [20]. For fatty acids alone, seven binding sites have been described [16].

Infrared spectroscopy provides measurements of molecular vibrations due to the specific absorption of infrared radiation by chemical bonds. It is known that the form and frequency of the Amide I band, which is assigned to the C=O stretching vibration within the peptide bonds is very characteristic for the structure of the studied protein [21]. From the band secondary structure, components peaks (α-helix, β-strand) can be derived and the analysis of this single band allows elucidation of conformational changes with high sensitivity.

This work will be limited to the mid-range infrared, which covers the frequency range from 4000 to 400 cm^{-1}. This wavelength region includes bands that arise from three conformational sensitive vibrations within the peptide backbone (Amides I, II and III) of these vibrations, Amide I is the most widely used and can provide information on secondary structure composition and structural stability. One of the advantages of infrared spectroscopy is that it can be used with proteins that are either in solution or in thin films. In addition, there is a growing body of literature on the use of infrared to follow reaction kinetics and ligand binding in proteins, as well as a number of infrared studies on protein dynamics.

Other spectroscopy techniques are usually used in studying the interaction of drugs and proteins, fluorescence and UV spectroscopy are commonly used because of their high sensitivity, rapidity and ease of implementation. Several reports have been published studying the interaction of proteins with drugs by fluorescence technique [22–26].

The binding of pentobarbital to HSA was investigated by means of UV-absorption spectroscopy, Fluorescence spectroscopy, and FT-IR spectroscopy. Spectroscopic evidence regarding the drug binding mode, drug binding constant and the effects of pentobarbital on the protein secondary structure are provided here.

2. Materials and methods

Pentobarbital in salt form and human serum albumin (fatty acid free) were purchased from Sigma chemical company and used without further purification.

2.1. Preparation of stock solutions

HSA was dissolved in phosphate buffered saline (80 mg/ml). The concentration of HSA in the buffer solution was prepared using its list molecular weight of 66.5 kDa. The solutions of pentobarbital with the following concentrations 0.015, 0.03, 0.06, 0.12, 0.24, 0.48, 0.96 mM were prepared by dissolving the drug in double distilled water. In the final step drug solution was added to an equal volume of the protein solution to attain the desired drug concentrations of 0.0075, 0.015, 0.03, 0.06, 0.12, 0.24, 0.48 mM with a final protein concentration of 4% w/v. The solution of pentobarbital and HSA were incubated for 1 h (at 20 °C) before spectroscopic measurements were taken.

2.2. UV-absorption spectra

The absorption spectra were obtained by the use of a NanoDrop ND-100 spectrophotometer. The absorption spectra were recorded for free HSA (40 mg/ml) and for its complexes with pentobarbital solutions with the concentrations of (0.75, 1.5, 3.0, 6.0, 12.0, 24.0, and 48.0) $\times 10^{-5}$ mol L^{-1}. Repeated measurements were done for all the samples and no significant differences were observed.

2.3. Fluorescence

The fluorescence measurements were performed by a NanoDrop® ND-3300 Fluorospectrometer at 25 °C. The excitation source comes from one of three solid-state light emitting diodes (LED's). The excitation source options include: UV LED with maximum excitation 365 nm, Blue LED with excitation 470 nm, and white LED from 500 to 650 nm excitation. A 2048-element CCD array detector covering 400–750 nm, is connected by an optical fiber to the optical measurement surface. The excitation is done at the wavelength of 360 nm and the maximum emission wavelength is at 439 nm.

2.4. FT-IR spectroscopic measurements

The FT-IR measurements were obtained on a Bruker IFS 66/S spectrophotometer equipped with a liquid nitrogen-cooled MCT detector and a KBr beam splitter. The spectrometer was continuously purged with dry air during the measurements. Samples are prepared after 2 h of incubation of HSA with pentobarbital solution at room temperature, four drops of the serum sample were placed on a certain area on a silicon window plate and left to dry at room temperature. The dehydrated films on one side of a silicon window plate of the samples containing different concentrations of pentobarbital with the same protein content.

The absorption spectra were obtained in the wave number range of 400–4000 cm^{-1}. A spectrum was taken as an average of 60 scans to increase the signal to noise ratio, and the spectral resolution was at 4 cm^{-1}. The aperture used in this study was 8 mm, since we found that this aperture gives best signal to noise ratio. Baseline correction, normalization and peak areas calculations were performed for all the spectra by OPUS software. The peak positions were determined using the second derivative of the spectra.

The infrared spectra of HSA and the pentobarbital–HSA complex were obtained in the region of 1000–1800 cm^{-1}. The FT-IR spectrum of free HSA was acquired by subtracting the absorption spectrum of the buffer solution from the spectrum of the protein solution. For the net interaction effect, the difference spectra {(protein and pentobarbital solution) – (protein solution)} were generated using the featureless region of the protein solution 1800–2200 cm^{-1} as an internal standard [27]. The accuracy of this subtraction method is tested using several control samples with the

same protein or drug concentrations, which resulted into a flat base line formation. The obtained spectral differences were used here, to investigate the nature of the drug–HSA interaction.

3. Results and discussion

3.1. UV-absorption spectroscopy

The pentobarbital–HSA binding constants were determined using UV-absorption spectroscopy as reported for several drug–protein complexes [28–30]. The absorption spectra for different concentration of pentobarbital in HSA are shown in Fig 2. Assuming only one type of interaction between pentobarbital and HSA in aqueous solution, leads to establish Eqs. (1) and (2) as follows:

$$\text{HSA} + \text{pentobarbital} \leftrightarrow \text{pentobarbital} : \text{HSA} \quad (1)$$

$$K = [\text{pentobarbital} : \text{HSA}]/[\text{pentobarbital}][\text{HSA}] \quad (2)$$

The absorption data were treated using linear reciprocal plots based on the following equation [31].

$$\frac{1}{A - A_0} = \frac{1}{A_\infty - A_0} + \frac{1}{K[A_\infty - A_0]} \cdot \frac{1}{L} \quad (3)$$

where A_0 corresponds to the initial absorption of protein at 280 nm in the absence of ligand, A_∞ is the final absorption of the ligated-protein, and A is the recorded absorption at different pentobarbital concentrations (L). The double reciprocal plot of $1/(A - A_0)$ vs. $1/L$ is linear (Fig. 3) and the binding constant (K) can be estimated from the ratio of the intercept to the slope to be $1.812 \times 10^4\ M^{-1}$. The binding constant value shows a relatively weak pentobarbital–HSA interaction in comparison to other drug–HSA complexes with binding constants in the range of 10^5 and $10^6\ M^{-1}$ [8]. The reason for the low stability can be attributed to the presence of mainly hydrogen-bonding interaction between protein donor atoms and the pentobarbital polar groups or an indirect drug–protein interaction through water molecules [24].

3.2. Fluorescence spectroscopy

The fluorescence of HSA results from the tryptophan, tyrosine, and phenylalanine residues. The intrinsic fluorescence of many proteins is mainly contributed by tryptophan alone, because phenylalanine has very low quantum yield and the fluorescence of tyrosine is almost totally quenched if it is ionized or near an amino group, a carboxyl group, or a tryptophan residue [32]. The fluorescence spectra of HSA at various concentrations of pentobarbital (0.75, 1.5, 3.0, 6.0, 12.0, 24.0, and 48.0) $\times 10^{-5}$ mol L^{-1} are shown in Fig. 4. The fluorescence intensity of HSA decreased regularly with the increasing of pentobarbital concentration, while the peak position shows little or no change at all.

The dynamic quenching process can be described by the Stern–Volmer equation [22]:

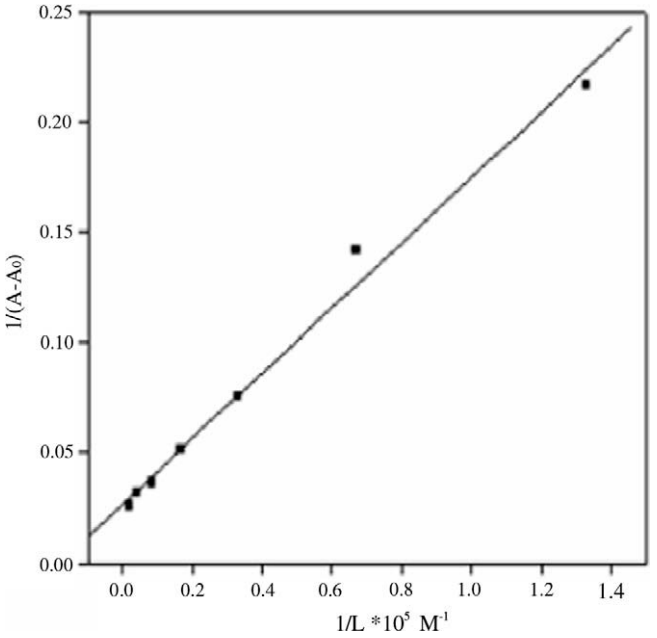

Fig. 3. The plot of $1/(A - A_0)$ vs. $1/L$ for HSA with different concentrations of pentobarbital.

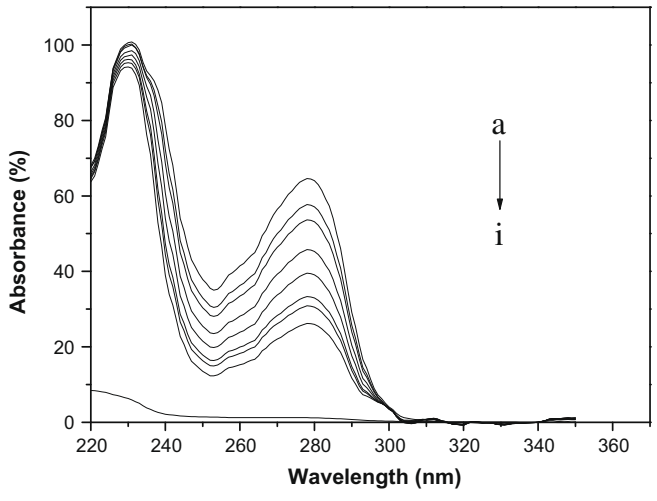

Fig. 2. UV-absorbance spectra of HSA with different concentrations of pentobarbital (a = 0.48 mM, b = 0.24 mM, c = 0.12 mM, d = 0.06 mM, e = 0.03 mM, f = 0.015 mM, g = 0.0075 mM, h = 0.0 mM, and i = pentobarbital).

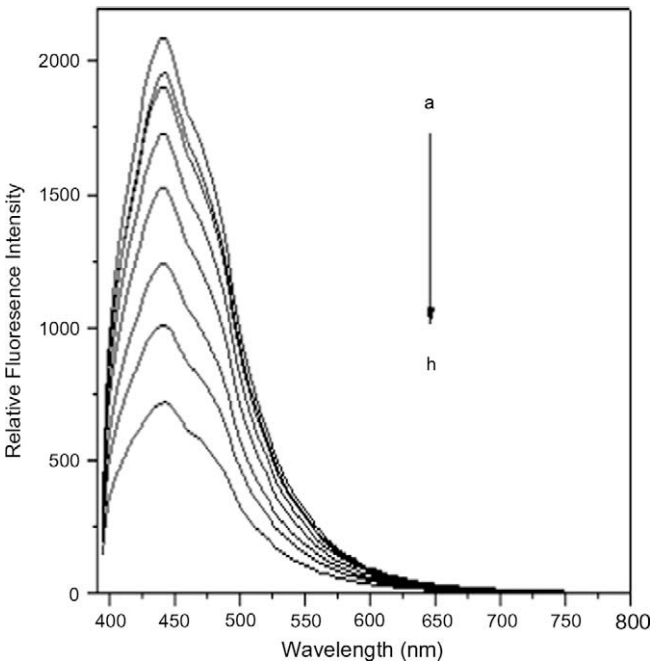

Fig. 4. Fluorescence emission spectra of HSA in the absence and presence of pentobarbital in these concentrations (a = 0.0 mM, b = 0.0075 mM, c = 0.015 mM, d = 0.03 mM, e = 0.06 mM, f = 0.12 mM, g = 0.24 mM, and h = 0.48 mM).

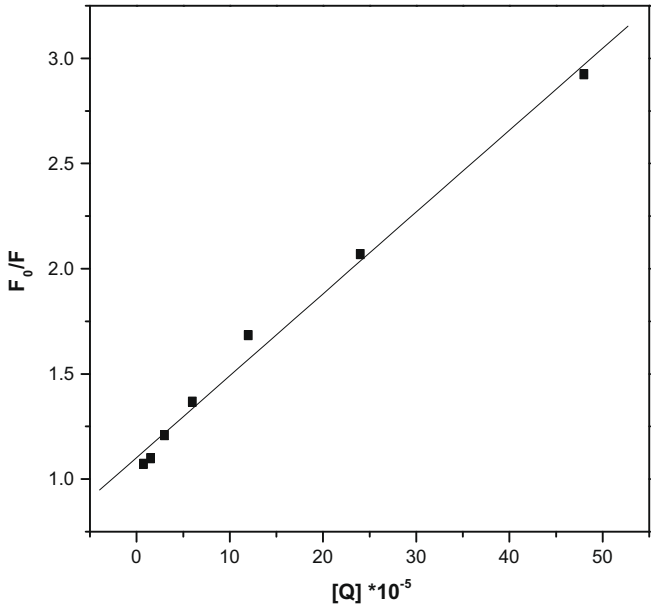

Fig. 5. The Stern–Volmer plot for pentobarbital–HSA system.

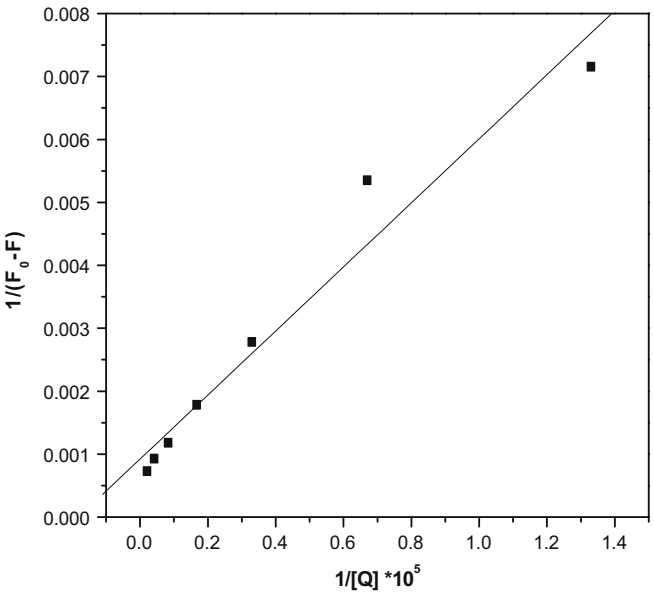

Fig. 6. The plot of $1/(F_0 - F)$ vs. $1/[Q \times 10^5]$.

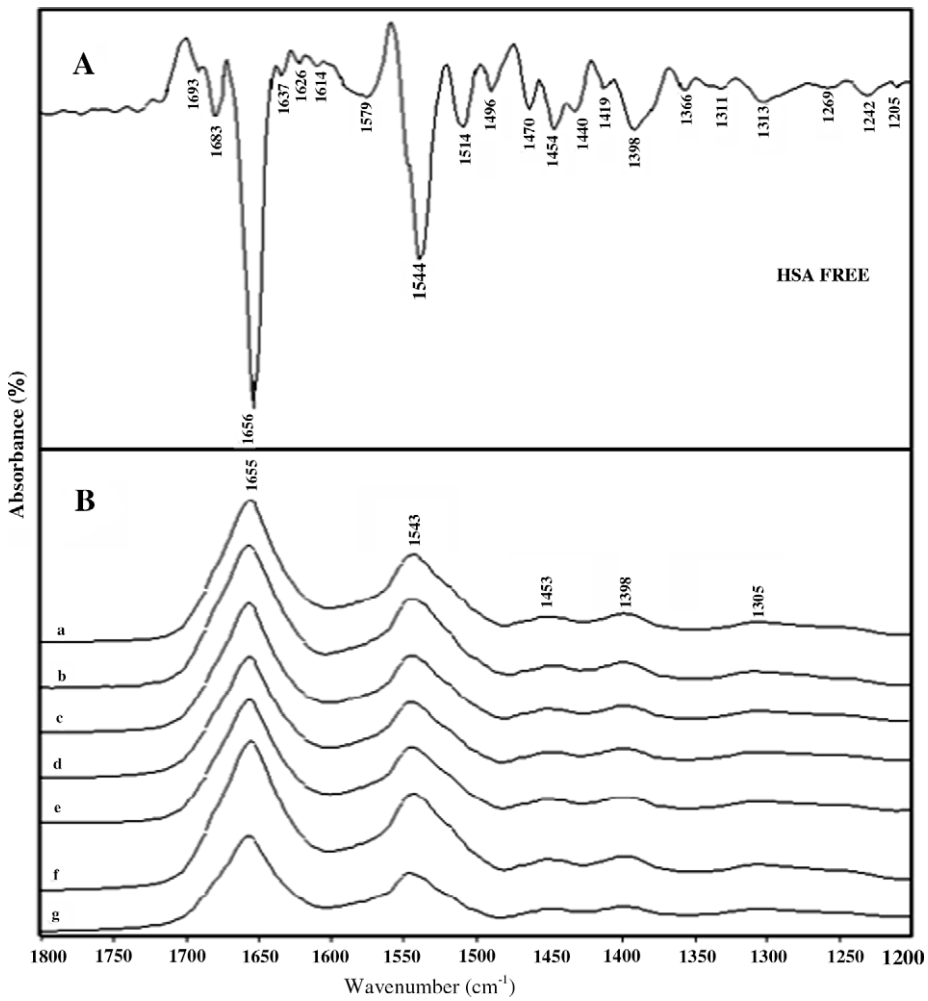

Fig. 7. The spectra of (A) HSA free (second derivative) and (a, b, c, d, e, f, and g) HSA–pentobarbital with concentrations (0.0, 0.0015, 0.003, 0.006, 0.012, 0.024, and 0.048 mM).

Table 1
Bands assignment in the absorbance spectra of HSA with different pentobarbital concentrations for Amide I–III regions.

Bands	HSA Free	HSA-Pento 0.015 mM	HSA-Pento 0.03 mM	HSA-Pento 0.06 mM	HSA-Pento 0.12 mM	HSA-Pento 0.24 mM	HSA-Pento 0.48 mM
Amide I	1614	1615	1614	1613	1613	1614	1612
(1600–1700)	1626	1627	1626	1626	1626	1626	1627
	1637	1637	1636	1637	1637	1636	1639
	1656	1657	1656	1656	1656	1654	1657
	1683	1680	1681	1682	1681	1682	1680
	1693	1691	1692	1693	1692	1694	1692
Amide II	1514	1515	1515	1515	1515	1515	1515
(1480–1600)	1532	1532	1532	1531	1531	1531	1532
	1544	1548	1546	1546	1546	1544	1548
	1564	1568	1570	1571	1570	1571	1568
	1579	1579	1582	1581	1581	1585	1584
	1594	1595	1595	1595	1595	1594	1596
Amide III	1226	1226	1226	1226	1226	1226	1226
(1220–1330)	1242	1243	1243	1243	1243	1242	1243
	1269	1267	1269	1268	1268	1268	1267
	1293	1292	1293	1294	1293	1293	1294
	1313	1312	1313	1314	1313	1313	1312

$$\frac{F_0}{F} = 1 + K_q \tau_0 (L) = 1 + K_{sv}(L) \quad (4)$$

where F and F_0 are the fluorescence intensities with and without quencher, K_q is the quenching rate constant of the biomolecule, K_{sv} is the Stern–Volmer quenching constant, τ_0 is the average lifetime of the biomolecule without quencher, and (L) is the concentration of pentobarbital. As can be seen from Fig. 5, the Stern–Volmer plot is linear and the slope is equal to K_{sv} (3.875×10^7 L mol^{-1}). Fluorescence quenching can be induced by different mechanisms, which were usually classified into dynamic quenching and static quenching. Dynamic quenching arises from Collisional encounters between the fluorophore and quencher, and static quenching resulting from the formation of a ground state complex between the fluorophore and the quencher [33].

The quenching rate constant K_q, can be calculated using the fluorescence life time of 10^{-8} s for HSA [34].

The obtained value of 3.875×10^{15} L mol^{-1} s^{-1} is much larger than the maximum dynamic quenching constant for various quenchers with biopolymer (2×10^{10} L mol^{-1} s^{-1}) [35]. This result confirms that a static quenching is dominant in the formed complexes [36]. When the static quenching equation is used [33]:

$$\frac{1}{F_0 - F} = \frac{1}{F_0 K(L)} + \frac{1}{F_0} \quad (5)$$

where K is the binding constant of pentobarbital with HSA. The value of K can be determined from the slope and the intercept in Fig. 6. The value of K is 1.809×10^4 M^{-1}, which agrees well with the value obtained earlier by UV spectroscopy and supports the effective role of static quenching. The highly effective quenching constant in this case has lead to a lower value of binding constant between the drug and HSA due to an effective hydrogen bonding between pentobarbital and HSA.

3.3. FT-IR spectroscopy

Infrared spectra of proteins exhibit a number of amide bands, which represent different vibrations of the peptide moiety. The amide group of proteins and polypeptides presents characteristic vibrational modes (amide modes) that are sensitive to the protein conformation and largely been constrained to group frequency interpretations [37]. Amide I (1700–1600 cm^{-1} region) is primarily due to the C=O stretching vibration, Amide II (1600–1480 cm^{-1} region) to the coupling of the N–H in-plane bending and C–N stretching modes, and Amide III (1330–1220 cm^{-1} region) to the C–N stretching coupled to the in-plane N–H bending mode [38–40]. Furthermore, other bands at 900–1300 cm^{-1} were assigned to C–O bending modes of saccharides (glucose, lactose and glycerol), the peaks at 1360–1430 cm^{-1} attributed to vibrations of certain

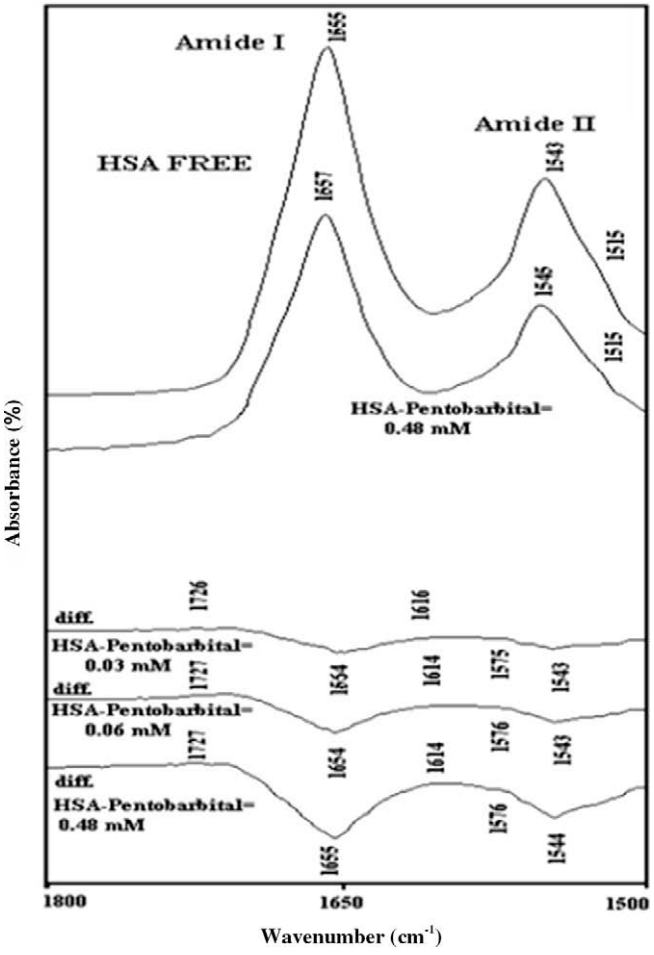

Fig. 8. FT-IR spectra (top two curves) and difference spectra of HSA and its complexes with different pentobarbital concentrations in the region of 1800–1500 cm^{-1}.

amino acids chains and 1430–1480 cm^{-1} is attributed to fatty acids, phospholipids and triglycerides [41,42].

The second derivative of the FT-IR spectrum for HAS free, and the spectra for HSA with different concentrations of pentobarbital are shown in Fig. 7, where the spectra are dominated by the absorbance bands of Amides I and II at 1655 and 1545 cm^{-1}, respectively. The peak positions of Amide I bands in HSA infrared spectrum shifted as listed in Table 1: 1615–1612 cm^{-1}, 1626–1627 cm^{-1}, 1683–1680 cm^{-1}, 1656–1657 cm^{-1} and 1693–1692 cm^{-1} after interaction with pentobarbital. In addition a peak at 1636 cm^{-1} has disappeared after the interaction with pentobarbital. The changes of these peak positions and peak shapes demonstrated the secondary structures of the HSA had been changed by the interaction of pentobarbital with HSA. In Amide II region some of the peak positions have shifted in the following order: 1544–1548 cm^{-1}, 1564–1568 cm^{-1} and 1594–1596 cm^{-1}. In the Amide III region little or no change of the peak positions has been observed. The minor changes in peak positions can be attributed to the effect of the newly imposed H-bonding between the drug molecules and the protein. It is suggested that, the shift to a higher frequency for the major peak in Amide1 region (1656–1657) came as a result of stabilization by hydrogen bonding by having the C–N bond assuming partial double bond character due to a flow of electrons from the C═O to the C–N bond [43].

The component bands of Amide I were attributed according to the well-established assignment criterion [44–45]. The bands range 1610–1640 cm^{-1} are generally assigned to β-sheet, 1640–1650 cm^{-1} to random coil, 1650–1658 cm^{-1} to α-helix and 1660–1700 cm^{-1} to β-turn structure. As for Amide II, the absorption band consists of four components and assigned in the following order: 1488–1500 cm^{-1} to β-sheets, 1504–1525 cm^{-1} to random coil, 1527–1560 cm^{-1} to α-helix and 1564–1585 cm^{-1} to turn structure [46]. The component bands of Amide III have been assigned as follows: α-helix 1330–1290 cm^{-1}, β-turn 1290–1270 cm^{-1}, random coil 1270–1250 cm^{-1} and β-sheet 1250–1220 cm^{-1}[45].

Most investigations have concentrated on Amide I band assuming higher sensitivity to the change of protein secondary structure [47]. However, it has been reported that the Amide II band has high information content and could be used alone for secondary structure prediction in place of Amide I [48–49]. Others have reported that Amide III is not directly affected by the strong water band and therefore it has been used for structure determinations [50].

The difference spectra [(protein + pentobarbital) – (protein)] were obtained to investigate the intensity variations and the results are shown in Fig. 8. Two strong negative features at 1654 and 1543 cm^{-1} were observed at low pentobarbital concentration (0.03 mM). These two negative features became even stronger at lower concentrations with a little shift in their positions. The observed negative features are attributed to the decrease of intensities at Amide I band at1654 and Amide II band at 1543 as a result of drug interaction (H-bonding) with protein C═O and C–N groups [24].

In this work, a quantitative analysis of the protein secondary structure for the free HSA and pentobarbital–HSA complex in dehydrated films is determined from the shape of Amide I, II and III bands. Infrared Fourier self-deconvolution with second derivative resolution and curve fitting procedures [51–52], were applied to increase spectral resolution and therefore to estimate the number, position and area of each component bands. The procedure was in general carried out considering only components detected by second derivatives and the half widths at half height (HWHH) for the component peaks are kept around 5 cm^{-1}. Based on the above assignments, the percentages of each secondary structure of HSA were calculated from the integrated areas of the component bands in Amides I, II and III, respectively. Table 2 shows the content of each secondary structure of HSA before and after the interaction with pentobarbital at different concentrations.

Table 2
Secondary structure determination for Amide I–III regions in HSA and its pentobarbital complexes.

Bands	HSA Free	HSA-Pento 0.015 mM	HSA-Pento 0.03 mM	HSA-Pento 0.06 mM	HSA-Pento 0.12 mM	HSA-Pento 0.24 mM	HSA-Pento 0.48 mM
Amide I							
β-Sheets (cm^{-1}) (1610–1640) (1680–1700)	16	18	16	18	17	17	19
Random (cm^{-1}) (1640–1650)	15	14	16	16	16	18	13
α-Helix (cm^{-1}) (1650–1660)	55	51	51	49	49	49	48
Turn (cm^{-1}) (1660–1680)	14	17	17	17	16	16	20
Amide II							
β-Sheets (cm^{-1}) (1488–1500) (1587–1598)	18	18	17	17	18	17	19
Random (cm^{-1}) (1504–1525)	14	11	12	14	13	14	10
α-Helix (cm^{-1}) (1527–1560)	50	50	51	48	50	50	47
Turn (cm^{-1}) (1564–1583)	18	21	20	21	19	19	24
Amide III							
β-Sheets (cm^{-1}) (1220–1254)	17	17	18	19	20	20	21
Random (cm^{-1}) (1258–1280)	15	16	15	16	15	16	16
Turn (cm^{-1}) (1283–1298)	18	18	18	17	17	17	17
α-Helix (cm^{-1}) (1298–1325)	50	49	49	48	48	47	46

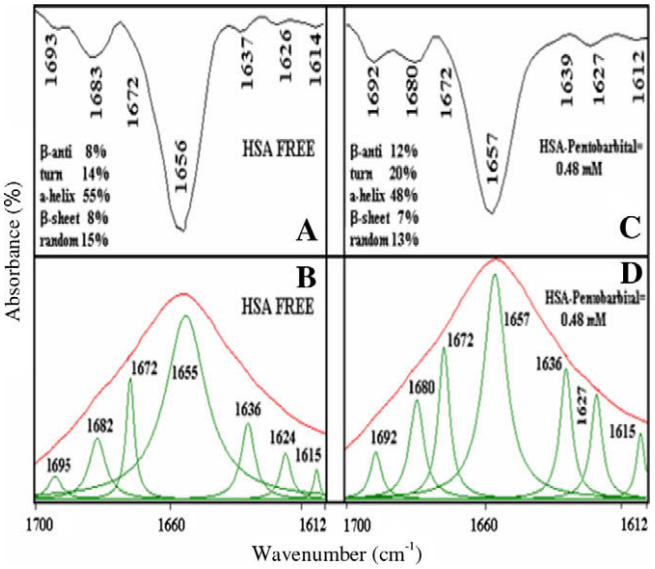

Fig. 9. Second-derivative resolution enhancement and curve-fitted Amide I region (1700–1612 cm^{-1}) and secondary structure determination of the free human serum albumin (A and B) and its pentobarbital complexes (C and D) with 0.48 mM drug concentration.

Fig. 9 reveals second derivative resolution enhancement and curve-fitted Amide I region and secondary structure determinations of the free human serum albumin (A and B) and its pentobarbital complexes (C and D) in dehydrated films. It is generally accepted that infrared spectra of proteins in films and in solution may display distinct differences, but these differences are due to the presence or absence of the water or buffer molecules that imprint their mark on the spectra. It has been shown that the structural information content is of the same quality in films and in solution with an (error of <1%) for both systems [53].

The percentage values for the components of Amide I of free HSA are consistent with the results of other recent spectroscopic studies [54–55]. The results of Amide II and Amide III showed similar trends in their percentage values to that of Amide I. The decrease of α-helix percentage with the increase of pentobarbital concentrations is evident in the calculations and this trend is consistent in the three Amide regions. However, for the β-sheet the relative percentage has increased with increasing pentobarbital concentrations. The reduction of α-helix intensity percentage in favour of the increase of β-sheets and turn structure are believed to be due to the unfolding of the protein in the presence of pentobarbital as a result of the formation of H-bonding between HSA and the drug. The steric blocking effect can contribute an enthalpic stabilization to intraprotein hydrogen bonds and disfavors peptide to catalyst complexation in hydrogen exchange reactions and peptide to peptide H-bonding in the helical main chain conformation but not in β-strands [56]. The newly formed H-bonding result in the C–N bond assuming partial double bond character due to a flow of electrons from the C=O to the C–N bond which decreases the intensity of the original vibrations [43]. It seems that the H-bonding effects more of the original bonding in α-helix than in β-sheets depending on the accessibility of the solvent and on propensities of α-helix and β-sheets of the protein [57]. The hydrogen bonds in α-helix are formed inside the helix and parallel to the helix axis, while for β-sheet the hydrogen bonds take position in the planes of β-sheets as the preferred orientations especially in the anti-parallel sheets. The restrictions on the formation of hydrogen bonds in β-sheet relative to the case in α-helix explain the larger effect on reducing the intensity percentage of α-helix to that of β-sheet. Similar conformational transitions from an α-helix to β-sheet structure were observed for the protein unfolding upon protonation and heat denaturation [58–59].

In summary, the binding of pentobarbital to HSA has been investigated by UV-absorption spectroscopy, fluorescence spectroscopy and by FT-IR spectroscopy. From the UV and Fluorescence Investigations, we determined values for the binding constant and the quenching constant. The results indicate that the intrinsic fluorescence of HSA was quenched by pentobarbital through static quenching mechanism. Analysis of the FT-IR spectra reveals that HSA–pentobarbital interaction induces intensity reduction in the absorption bands of α-helix and β-sheets components with different proportionality due to the different accessibility of H-bond formation in these components.

Acknowledgement

This work is supported by the German Research Foundation DFG Grant No. DR228/24-2.

References

[1] C. Donald, Essentials of Pharmaceutical Chemistry, Pharmaceutical Press, London, 2003 (Chapter 1).
[2] B.E. Hetzer, L.K. Krekow, Neurotoxicol. Teratol. 21 (1999) 181.
[3] J.E. Hodes, T.T. Soncrant, D.M. Larson, S.G. Carlson, S.I. Rapoport, Anesthesiology 63 (1985) 633.
[4] T. Peters, Adv. Protein Chem. 37 (1985) 161.
[5] X.M. He, D.C. Carter, Nature 358 (1992) 209.
[6] S. Curry, P. Brick, N.P. Franks, Biochim. Biophys. Acta 1441 (1999) 131.
[7] F. Herve, S. Urien, E. Albengres, J.C. Duche, J. Tillement, Clin. Pharmacokinet. 26 (1994) 44.
[8] U. Kragh-Hansan, Pharmacol. Rev. 33 (1981) 17.
[9] P.B. Kandagal, S.M.T. Shaikh, D.H. Manjunatha, J. Seetharamappa, B.S. Nagaralli, J. Photochem. Photobiol. A 189 (2007) 121.
[10] K. Oettl, R.E. Stauber, Br. J. Pharmacol. 151 (2007) 580.
[11] U. Kragh-Hansen, V.T.G. Chuang, M. Otagiri, Biol. Pharm. Bull. 25 (2002) 695.
[12] G. Sudlow, D.J. Birkett, D.N. Wade, Mol. Pharmacol. 11 (1975) 824.
[13] F. Shin-ichi, A. Takashi, Biophys. J. 94 (2008) 95.
[14] K.H. Ulrich, W. Hiroshi, N. Keisuke, I. Yasunori, O. Masaki, J. Mol. Biol. 363 (2006) 702.
[15] A. Bhattacharya, T. Gruene, S. Curry, J. Mol. Biol. 303 (2000) 721.
[16] J.R. Simard, P.A. Zunszain, J.A. Hamilton, S. Curry, J. Mol. Biol. 361 (2006) 336.
[17] S.S. Krishnakumar, D. Panda, Biochemistry 41 (2002) 7443.
[18] Y.V. Il'ichev, J.L. Perry, J.D. Simon, J. Phys. Chem. B 106 (2002) 460.
[19] T. Peters, All about Albumin, Academic Press, San Diego, 1995 (Chapter 3).
[20] U. Kragh-Hansen, Dan. Med. Bull. 37 (1990) 57.
[21] S. Krimm, J. Bandekar, Adv. Protein Chem. 38 (1986) 181.
[22] J.N. Tian, J.Q. Liu, J.Y. Zhang, Z.D. Hu, X.G. Chen, Chem. Pharm. Bull. 51 (2003) 579.
[23] J. Sereikaite, V.A. Bumelis, Acta Biochim. Pol. 53 (2006) 87.
[24] M. Purcell, J.F. Neault, H.A. Tajmir-Riahi, Biochim. Biophys. Acta 1478 (2000) 61.
[25] T. Jianghong, L. Ning, H. Xianghong, Z. Guohua, J. Mol. Struct. 889 (2008) 408.
[26] J. Li, C. Ren, Y. Zhang, X. Liu, X. Yao, Z. Hu, J. Mol. Struct. 881 (2008) 90.
[27] W.K. Surewicz, H.H. Mantsch, D. Chapman, Biochemistry 32 (1993) 389.
[28] J.J. Stephanos, J. Inorg. Biochem. 62 (1996) 155.
[29] M.I. Klotz, L.D. Hunston, Biochemistry 10 (1971) 3065.
[30] I.M. Klotz, Science 217 (1982) 1247.
[31] J. Stephanos, S. Farina, A. Addison, Biochem. Biophys. Acta 1295 (1996) 209.
[32] A. Sulkowaska, J. Mol. Strurct. 614 (2002) 227.
[33] J.R. Lakowicz, Principles of Fluorescence Spectroscopy, Kluwer Academic Publishers/Plenum Press, Dordrecht/New York, 1999 (Chapter 8).
[34] G.Z. Chen, X.Z. Huang, J.G. Xu, Z.Z. Zheng, Z.B. Wang, Method of Fluorescence Analysis, Science Press, Beijing, 1990 (Chapter 4).
[35] J.R. Lakowicz, G. Weber, Biochemistry 12 (1973) 4161.
[36] T. Wang, B. Xiang, Y. Wang, C. Chen, Y. Dong, H. Fang, M. Wang, Colloids Surf. B 65 (2008) 113.
[37] Z. Ganim, A. Tokmakoff, Biophys. J. 91 (2006) 2636.
[38] V.A. Sirotkin, A.N. Zinatullin, B.N. Solomonov, D.A. Faizullin, V.D. Fedotov, Biochim. Biophys. Acta 1547 (2001) 359.
[39] R.K. Dukor, J.M. Chalmers, P.R. Griffiths (Eds.), Vibrational Spectroscopy in the Detection of Cancer, Handbook of Vibrational Spectroscopy, vol. 5, Wiley, Chichester, 2001 (Chapter 3).
[40] Y.N. Chirgadze, O.V. Fedorov, N.P. Trushina, Biopolymers 14 (1975) 679.
[41] G. Deleris, C. Petibios, Vib. Spectrosc. 32 (2003) 129.
[42] E. Bramanti, E. Benedetti, Biopolymers 38 (1996) 639.
[43] M. Jackson, H.H. Mantsch, J. Chem. 69 (1991) 1639.
[44] D.M. Byler, J.N. Brouilette, H. Susi, Spectroscopy 1 (1986) 39.

[45] M. Jiang, M.X. Xie, D. Zheng, Y. Liu, X.Y. Li, X. Chen, J. Mol. Struct. 692 (2004) 71.
[46] A.I. Ivanov, R.G. Zhbankov, E.A. Korolenko, E.V. Korolik, L.A. Meleshchenko, M. Marchewka, H. Ratajczak, J. Appl. Spectrosc. 60 (1994) 305.
[47] K. Rahmelow, W. Hubner, Anal. Biochem. 241 (1996) 5.
[48] G. Erik, R. Jean-Marie, R. Vincent, Biophys. J. 90 (2006) 2946.
[49] K.A. Oberg, J.M. Ruysschaert, E. Goormaghtigh, Eur. J. Biochem. 271 (2004) 2937.
[50] F.N. Fu, D.B. DeOliveira, W.R. Trumble, H.K. Sarkar, B.R. Singh, Appl. Spectrosc. 48 (1994) 1432.
[51] M. Byler, H. Susi, Biopolymers 25 (1986) 469.
[52] E. Goormaghtigh, V. Cabiaux, J.M. Ruysschaert, Eur. J. Biochem. 193 (1990) 409.
[53] E. Goormaghtigh, V. Raussens, J.M. Ruysschaert, Biochim. Biophys. Acta 1422 (1999) 105.
[54] A. Ahmed Ouameur, E. Mangier, S. Diamantoglou, R. Rouillon, R. Carpentier, H.A. Tajmir-Riahi, Biopolymers 73 (2004) 503.
[55] R. Beauchemin, C.N. N'soukpoe -Kossi, T.J. Thomas, T. Thomas, R. Carpentier, H.A. Tajmir-Riahi, Biomacromolecules 8 (2007) 3177.
[56] Y. Bai, S.W. Englander, Proteins 18 (1994) 262.
[57] C.A. Kim, J.M. Berg, Nature 362 (1993) 267.
[58] F.S. Parker, Applications of Infrared, Raman, and Resonance Raman Spectroscopy in Biochemistry, Plenum Press, New York, 1983 (Chapter 3).
[59] I.E. Holzbaur, A.M. English, A.A. Ismail, Biochemistry 35 (1996) 5488.